JOURNAL OF AGRICULTURAL AND FOOD CHEMISTRY

Article

pubs.acs.org/JAFC

Antibacterial Electrospun Poly(lactic acid) (PLA) Nanofibrous Webs Incorporating Triclosan/Cyclodextrin Inclusion Complexes

Fatma Kayaci,[†] Ozgun C. O. Umu,[†] Turgay Tekinay,[†,‡] and Tamer Uyar*,[†]

[†]UNAM-Institute of Materials Science and Nanotechnology, Bilkent University, Ankara 06800, Turkey

[‡]Life Sciences Application and Research Center, Gazi University, Ankara 06830, Turkey

ABSTRACT: Solid triclosan/cyclodextrin inclusion complexes (TR/CD-IC) were obtained and then incorporated in poly(lactic acid) (PLA) nanofibers via electrospinning. α-CD, β-CD, and γ-CD were tested for the formation of TR/CD-IC by a coprecipitation method; however, the findings indicated that α-CD could not form an inclusion complex with TR, whereas β-CD and γ-CD successfully formed TR/CD-IC crystals, and the molar ratio of TR to CD was found to be 1:1. The structural and thermal characteristics of TR/CD-IC were investigated by ^{1}H NMR, FTIR, XRD, DSC, and TGA studies. Then, the encapsulation of TR/β-CD-IC and TR/γ-CD-IC in PLA nanofibers was achieved. Electrospun PLA and PLA/TR nanofibers obtained for comparison were uniform, whereas the aggregates of TR/CD-IC crystals were present and distributed within the PLA fiber matrix as confirmed by SEM and XRD analyses. The antibacterial activity of these nanofibrous webs was investigated. The results indicated that PLA nanofibers incorporating TR/CD-IC showed better antibacterial activity against *Staphylococcus aureus* and *Escherichia coli* bacteria compared to PLA nanofibers containing only TR without CD-IC. Electrospun nanofibrous webs incorporating TR/CD-IC may be applicable in active food packaging due to their very high surface area and nanoporous structure as well as efficient antibacterial property.

KEYWORDS: *cyclodextrin, inclusion complex, electrospinning, nanofiber, poly(lactic acid) (PLA), triclosan*

INTRODUCTION

Electrospinning is a cost-effective and versatile technique that is used for fabricating functional nanofibers and nanofibrous webs from a wide variety of materials including polymers, sol−gels, and composite structures.[1−5] Due to their unique properties, such as very large surface area-to-volume ratio and nanoporous feature, nanofibrous membranes based on electrospun nanofibers are suitable candidates for use in filtration, health care, textiles, energy, sensors, and so on.[1−6] Electrospun nanofibers and their nanowebs have also shown some potential in biotechnology and active food packaging, because active additives such as antibacterials,[6] antioxidants,[7] essential oils,[8] or even probiotics[9] can be effectively encapsulated into an electrospun nanofibrous matrix.

Cyclodextrins (CDs) are naturally occurring nontoxic cyclic oligosaccharides consisting of α-1,4-linked glucopyranose units.[10−12] There are three most common native CD types, α-CD, β-CD, and γ-CD, which have six, seven, and eight glucopyranose units in the cyclic structure, respectively. CDs have a unique truncated cone-shaped molecular structure. The size of the CD cavity is in the order γ-CD > β-CD > α-CD, whereas the cavity depth of the CD is same, which ∼8 Å is (Figure 1a).[13] CDs have a unique ability to form inclusion complexes (IC) with a variety of guests such as drugs, antibacterials, food additives, and textile auxiliaries, and inclusion complexation can enhance stability, solubility, bioavailability, functionality, and controlled/sustained release of these guest molecules.[10−19] Hence, the functionalization of electrospun nanofibers with CD-IC is extremely attractive, because such nanofibers have specific functions obtained by combining the exclusive properties of both nanofibers and CD-IC. Recently, we have shown that prolonged shelf life and high temperature stability for volatile additives such as menthol[20−22] and vanillin[23] can be achieved by their CD inclusion complexes incorporated into electrospun nanofibers.

Here, we first tried to form solid triclosan/cyclodextrin inclusion complexes (TR/CD-IC) by using three types of CD (α-CD, β-CD, γ-CD). Triclosan (TR) is a practically water-insoluble antibacterial agent; therefore, its antibacterial activity can be enhanced by increasing the solubility by forming CD-IC.[24−29] Then, the prepared TR/CD-IC were incorporated in poly(lactic acid) (PLA) nanofibers via electrospinning. PLA is a well-known biodegradable, biocompatible, and nontoxic natural polymer used in food packaging.[30−32] The antibacterial properties of the resulting PLA/TR/CD-IC electrospun nanofibrous webs were investigated against Gram-positive bacteria (*Staphylococcus aureus*) and Gram-negative bacteria (*Escherichia coli*). The encapsulation of TR/CD-IC in the PLA nanofiber matrix yielded an enhanced bacteriocidal efficacy compared to PLA/TR nanofibers without CD-IC. Therefore, antibacterial PLA nanofibrous webs incorporating TR/CD-IC can be applicable in active food packaging.

MATERIALS AND METHODS

Materials. PLA, a commercial polylactide resin identified as Ingeo biopolymer, was donated by NatureWorks LLC Co. (product code 4043D). TR (≥97% (HPLC), Sigma-Aldrich), *N*,*N*-dimethylformamide (DMF; Pestanal, Riedel), chloroform (99−99.4% (GC), Sigma-Aldrich), and deuterated dimethyl sulfoxide (DMSO-d_6, deuteration

Received: January 30, 2013
Revised: April 2, 2013
Accepted: April 3, 2013
Published: April 4, 2013

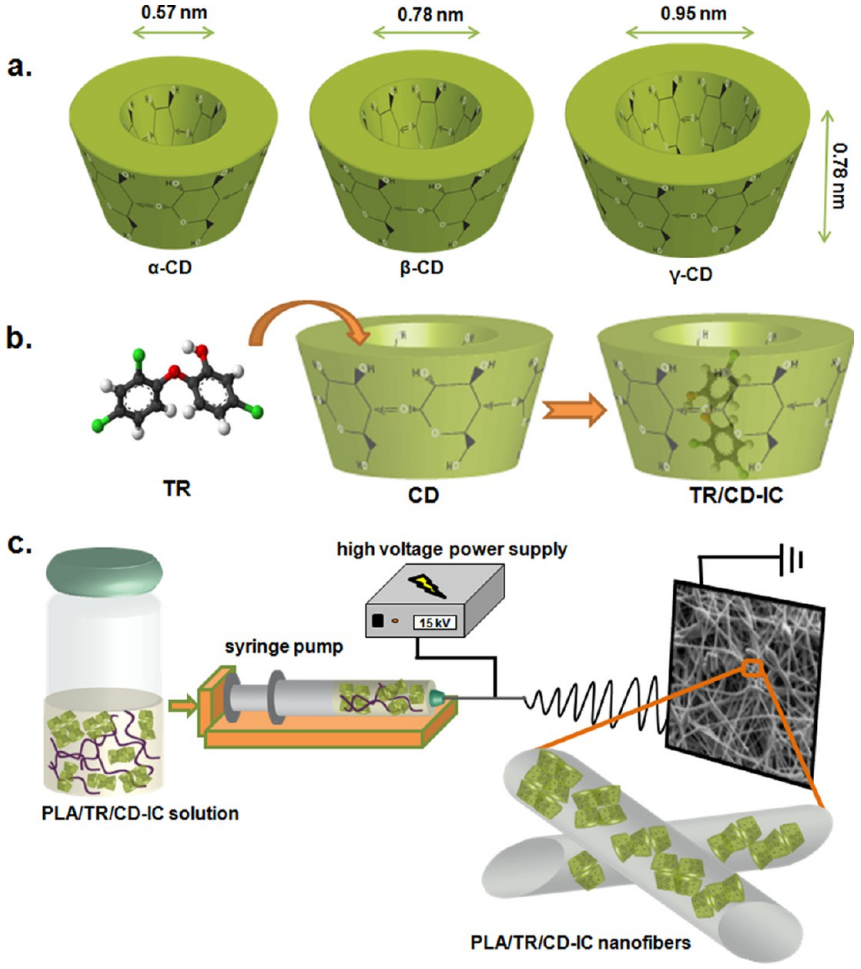

Figure 1. (a) Approximate dimensions of α-CD, β-CD, and γ-CD; schematic representations of (b) formation of TR/CD-IC and (c) electrospinning of PLA/TR/CD-IC solution.

Table 1. Solution Compositions and Morphological Characteristics of Resulting Electrospun Nanofibers and Inhibition Zone Results Taken after 24 h of Incubation at 37 °C against *E. coli* and *S. aureus* Bacteria for PLA/TR, PLA/TR/β-CD-IC, and PLA/TR/γ-CD-IC

					fiber diameter (nm)			zone of inhibition diameter (cm)	
solution	% PLA[a] (w/v)	% TR/CD-IC[b] (w/w)	% TR[b] (w/w)	viscosity (Pa·s)	range	average	fiber morphology	*E. coli*	*S. aureus*
PLA	8			0.106	140−900	650 ± 160	bead-free nanofibers		
PLA/TR	8		5	0.115	250−950	560 ± 150	bead-free nanofibers	3.0 ± 0.20	2.83 ± 0.28
PLA/TR/β-CD-IC	8	44	5	0.135	210−1580	640 ± 480	nanofibers with CD-IC crystals	3.7 ± 0.15	3.50 ± 0.00
PLA/TR/γ-CD-IC	8	50	5	0.176	260−2070	940 ± 500	nanofibers with CD-IC crystals	3.3 ± 0.00	2.90 ± 0.17

[a]With respect to solvent (chloroform/DMF, 9:1 (v/v)). [b]With respect to polymer (PLA).

degree minimum 99.8% for NMR spectroscopy, Merck) were purchased. Cyclodextrins (α-CD, β-CD, and γ-CD) were purchased from Wacker Chemie AG. All of these materials were used as-received. The water used as solvent was obtained from a Millipore Milli-Q ultrapure water system.

Preparation of Solid Triclosan/Cyclodextrin Inclusion Complexes. The formation of solid inclusion complexes (IC) of TR with α-CD, β-CD, and γ-CD was performed by a coprecipitation method. In all cases, the molar ratio of TR to CD used was 0.5:1. Initially, 0.149 g (5.1×10^{-4} mol), 0.128 g (4.4×10^{-4} mol), and 0.112 g (3.9×10^{-4} mol) of TR were stirred in 2 mL of water, individually, for the IC formation of TR with α-CD, β-CD, and γ-CD, respectively. Because TR is not water-soluble, a suspension was obtained in each vial. Then, 1 g of α-CD (1×10^{-3} mol), β-CD (8.8×10^{-4} mol), and γ-CD (7.8×10^{-4} mol) was dissolved in 4.9, 52, and 2.3 mL of water at 60 °C, respectively. The total amount of water used was determined according to the solubility of CD in water at 25 °C, that is, 14.5, 1.85, and 23.2 g/100 mL for α-CD, β-CD, and γ-CD, respectively.[10,13] The resulting CD solution was added into the aqueous TR suspension dropwise. Finally, each TR/CD solution was mixed at 60 °C for 1 h and then stirred overnight at room temperature. TR/α-CD solution was not turbid subsequent to stirring overnight, and TR particles were suspended, indicating that TR did not form an inclusion complex with α-CD; therefore, we eliminated the use of TR/α-CD in this study. On the other hand, turbid TR/β-CD and TR/γ-CD solutions were obtained after mixing overnight, and precipitation was observed for both of these solutions, elucidating the

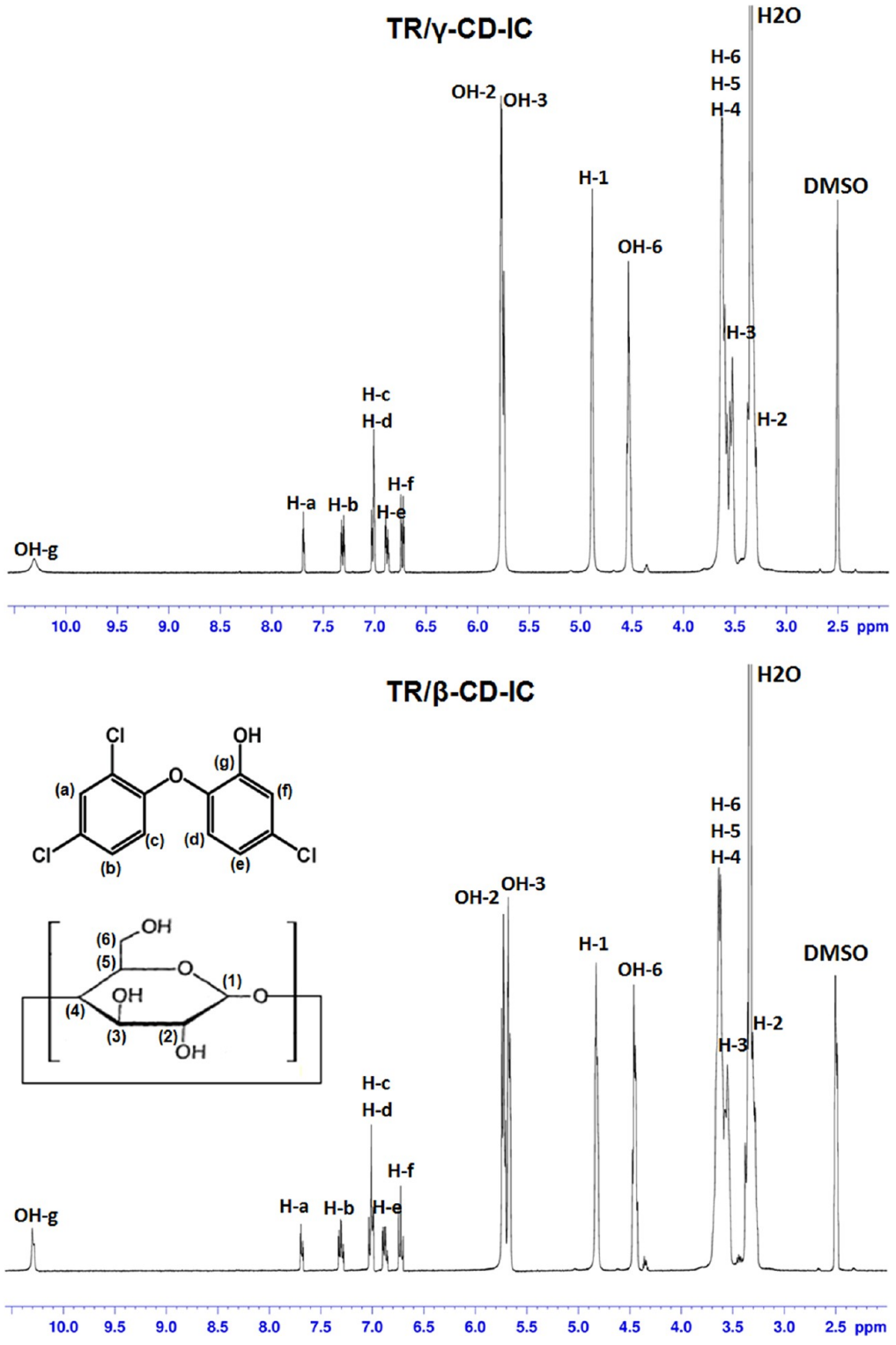

Figure 2. ^{1}H NMR spectra of TR/CD-IC dissolved in DMSO-d_6.

formation of inclusion complexes between TR and β-/γ-CD. The resulting TR/CD suspensions were filtered by using a borosilicate filter (por. 3) to obtain solid TR/CD-IC. The filtrate was washed with water several times to remove uncomplexed CD and then dried overnight under the hood. Finally, the solid TR/β-CD-IC and TR/γ-CD-IC were crushed in a mortar to obtain a fine white powder and weighed about 0.59 and 0.60 g, respectively. The yield was around 50%, because an excess amount of CD was used for the complexation (molar ratio of TR to CD was 0.5:1). From the NMR study as discussed in a later section, it was found that the complexation molar ratio of TR to CD was 1:1; therefore, the uncomplexed CD molecules did not precipitate and/or might be removed from the samples during the washing and filtration process.

Preparation of the Solutions Used for Electrospinning. TR/β-CD-IC and TR/γ-CD-IC were incorporated in PLA nanofibers via electrospinning. The amount of TR/β-CD-IC (44%, w/w) and TR/γ-CD-IC (50%, w/w) was adjusted to include 5% (w/w) TR with respect to PLA content. First, the TR/CD-IC crystals were dispersed in a

dx.doi.org/10.1021/jf400440b | J. Agric. Food Chem. 2013, 61, 3901−3908

chloroform/DMF (9:1, v/v) solvent system by stirring for 30 min at room temperature. Then PLA was added to these dispersions and completely dissolved by mixing for 5 h at room temperature. On the other hand, we have also prepared solutions of PLA and PLA/TR without CD under the same conditions for comparison. PLA and PLA/TR solutions were clear and transparent, whereas PLA/TR/CD-IC solutions were turbid due to the dispersion of TR/CD-IC crystals within the PLA solution. For all solutions, the PLA concentration was 8% (w/v) with respect to solvent (chloroform/DMF (9:1, v/v)). Table 1 summarizes the compositions of these solutions used for the electrospinning.

Electrospinning. Each prepared solution was placed in a 10 mL syringe fitted with a metallic needle having a 0.55 mm inner diameter and an 0.8 mm outer diameter, and the syringe was fixed horizontally on the syringe pump (KD Scientific, model 101). The electrode of the high-voltage power supply (Matsusada Precision, AU Series) was clamped to the metal needle tip, whereas the stationary cylindrical collector covered by a piece of aluminum foil was grounded. Tip-to-collector distance was kept at 10 cm, and the solutions were pumped with a flow rate of 1 mL/h. When a voltage of +15 kV was applied to the metal needle tip, the nanofibers were deposited on the collector. The electrospinning apparatus was in an enclosed Plexiglas box, and the electrospinning was performed at 24 °C and 20% relative humidity. The collected nanofibers were left in the suction hood at room temperature for 24 h to remove the residual solvent if any was present.

Characterizations and Measurements. Characterizations of solid TR/CD-IC were carried out by proton nuclear magnetic resonance (^{1}H NMR), Fourier transform infrared (FTIR) spectroscopy, X-ray diffraction (XRD), differential scanning calorimetry (DSC), and thermogravimetric analyzer (TGA). Pure triclosan and as-received CD were also characterized for comparison. To determine the stoichiometries of the TR/CD, ^{1}H NMR (DPX-400, Bruker) spectra were recorded at 400 MHz and 25 °C by dissolving about 20 g/L sample in DMSO-d_6. For FTIR analyses, a small amount of sample was mixed with potassium bromide (KBr, FTIR grade) in a mortar, and then a pellet was obtained using a press by applying high pressure. The infrared spectra of the samples were obtained by using FTIR spectroscopy (Bruker-VERTEX 70). The FTIR spectra were recorded from 750 to 1800 cm^{-1}, at a resolution of 4 cm^{-1}, by taking 64 scans for each sample. XRD (PANalyticalX'Pert Powder diffractometer) data of the samples were obtained by using Cu Kα radiation in a range of 2θ = 5−30°. DSC (Q2000, TA Instruments) and TGA (Q500, TA Instruments) were used to investigate the thermal properties of the samples. DSC analyses were carried out under nitrogen (N_2) atmosphere; the samples were equilibrated at 0 °C and then heated to 200 °C with a heating rate of 20 °C/min. TGA analyses were performed from room temperature to 450 °C at a 20 °C/min heating rate, and N_2 was used as a purge gas. The viscosity of the solutions used for electrospinning was measured by using a Rheometer (Physica MCR 301, Anton Paar) equipped with a cone/plate accessory (spindle type CP 40-2) at 22 °C, with a constant shear rate of 100/s. A scanning electron microscope (SEM) (Quanta 200 FEG, FEI) was used for the morphological investigation of electrospun nanofibers. Prior to SEM imaging, nanofiber samples were sputtered with 5 nm Au/Pd (PECS-682). Around 100 fiber diameters were measured from the SEM images to calculate the average fiber diameter (AFD) and to determine the fiber diameter range of each sample. XRD data of the nanofibers were also recorded in a range of 2θ = 5−30°.

Antibacterial Activity Test. The antibacterial properties of the electrospun nanofibrous webs were investigated against Gram-positive bacteria, *S. aureus* (ATCC 25923), and Gram-negative bacteria, *E. coli* (RSHM 888, National Type Culture Collection Laboratory, Ankara, Turkey). This test was done in vitro using a disk agar diffusion method. One hundred microliters of the cultures that contain 10^{12}/mL *S. aureus* or 5×10^{12}/mL *E. coli* was spread onto LB agar. The samples, which are named PLA/TR, PLA/TR/β-CD-IC, and PLA/TR/γ-CD-IC, were cut into circular disks having a diameter of about 1 cm. Then the nanofibrous webs were put on the agar, the agar plates were incubated at 37 °C for 24 h, and the inhibition zone diameters were measured.

RESULTS AND DISCUSSION

In this study, we aimed to prepare solid CD-IC with TR by using three types of CDs (α-CD, β-CD, and γ-CD). The formation of inclusion complexes between α-CD and TR was unsuccessful possibly because of the small cavity size of α-CD, which is not a suitable host for the guest TR molecules or because the chosen experimental conditions and the aqueous solvent system were not appropriate to form the CD-IC. However, the formation of inclusion complexes between β-CD and TR (TR/β-CD-IC) and between γ-CD and TR (TR/γ-CD-IC) was successful, and solid white powders of TR/β-CD-IC and TR/γ-CD-IC were obtained by filtration. The schematic representations of the formation of TR/CD-IC and electrospinning of PLA solution incorporating TR/CD-IC (PLA/TR/CD-IC) are indicated in Figure 1b,c.

The molar stoichiometry of TR/CD in the solid TR/β-CD-IC and TR/γ-CD-IC was determined by ^{1}H NMR (Figure 2). Initially, a ^{1}H NMR study was performed for pure CD and TR to detect the characteristic peaks corresponding to their protons, and it was observed that the peaks for TR were not overlapped with the peaks of CD (data not shown). The stoichiometry of the CD and TR in the CD-IC samples was calculated by taking the integrations of the CD peak at 4.8 ppm (H-1) and of the TR peak at 7.3 ppm (H-b). It was found that the stoichiometric ratios of TR to β-CD and TR to γ-CD were around 1:1 for TR/β-CD-IC and TR/γ-CD-IC samples. At the beginning, an excess amount of CD was used (initial molar ratio of TR to CD of 0.5:1) for the complexation process; however, the molar ratio of TR to CD was found to be 1:1 for TR/CD-IC samples.

The chemical structures of TR/CD-IC samples were investigated by FTIR spectroscopy, and pure TR and CD were also studied for comparison (Figure 3). The characteristic absorption peaks of pure CD were observed at around 1030, 1080, and 1157 cm^{-1} due to the coupled C−C/C−O stretching vibrations and the asymmetric stretching vibration of the C−O−C glycosidic bridge.[14] The FTIR spectrum of pure TR exhibited three characteristic peaks at 1505, 1472, and 1418 cm^{-1} corresponding to skeletal vibrations relating C−C stretching in the benzene ring.[24] Additionally, the peaks in the region from 1300 to 1000 cm^{-1} and from 900 to 750 cm^{-1} in the spectrum of pure TR were consequent of in-plane and out-of-plane bending of the aromatic ring C−H bonds, respectively, whereas the peaks at 1102 and 1084 cm^{-1} were related to C−Cl absorption.[24] In the case of TR/β-CD-IC and TR/γ-CD-IC samples, characteristic peaks of TR and CD were observed, confirming the presence of both TR and CD in these samples. In addition, the characteristic peaks of TR at 1505, 1472, and 1418 cm^{-1} shifted to 1507, 1474, and 1419 cm^{-1}, respectively, for the TR/CD-IC samples. This suggests host−guest interactions between CD and TR, because inclusion complexation causes FTIR peak shifts as also reported for TR/CD-IC samples in the literature.[27,33]

The crystalline structures of the CD-IC (TR/β-CD-IC and TR/γ-CD-IC), pure TR, and CD were investigated by XRD. The XRD patterns of as-received β-CD and γ-CD (Figure 4a) showed characteristic diffraction peaks in the range of 2θ = 5−30° for a cage-type packing structure, which are consistent with the literature findings.[34,35] The inclusion complexation generally confirmed the characteristic XRD peaks of CD molecules having channel-type arrangement in which CD molecules are aligned and stacked on top of each other by forming cylindrical channels.[34,35] Moreover, XRD patterns of CD-IC show no diffraction peaks of guest molecules, which are isolated from each other by the CD cavities and therefore cannot form crystals.[14,33]

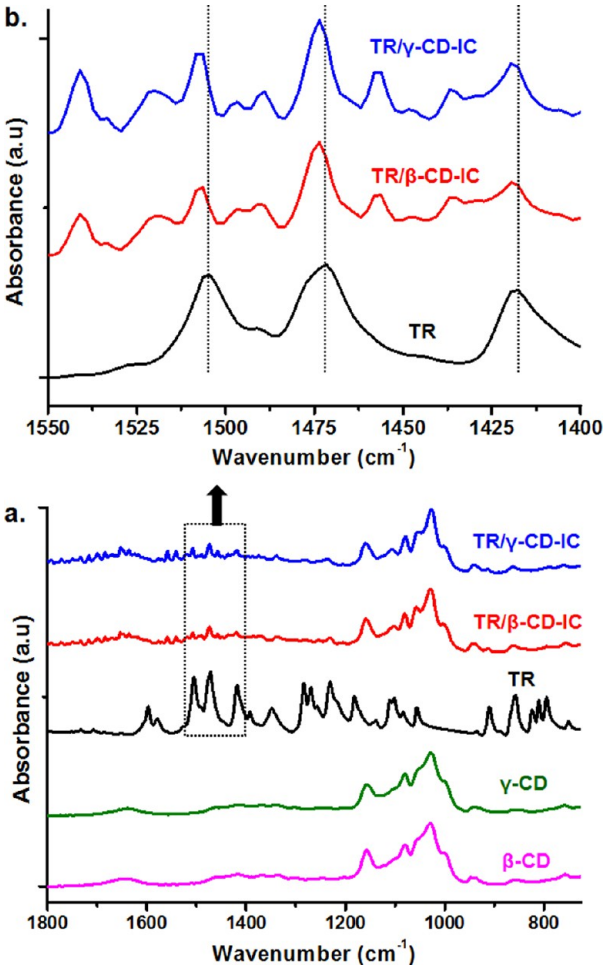

Figure 3. (a) FTIR spectra of as-received CD, pure TR, and solid TR/CD-IC and (b) enlarged region of FTIR spectra between 1550 and 1400 cm^{-1} of pure TR and solid TR/CD-IC.

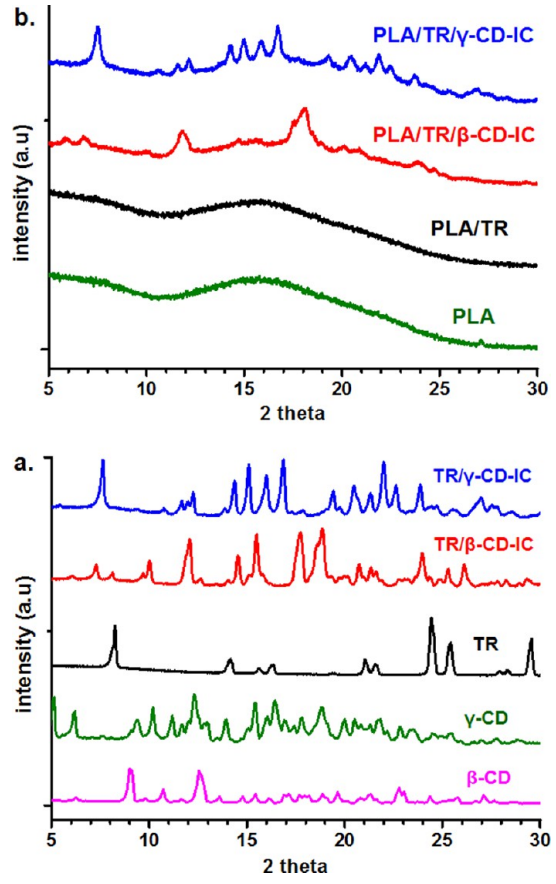

Figure 4. XRD patterns of (a) as-received CD, pure TR, and solid TR/CD-IC and (b) the resulting electrospun nanowebs.

TR is a crystalline material, and the XRD pattern of TR has major diffraction peaks at $2\theta \cong 8.2°$, 24.4°, and 25.4° (Figure 4a). The peaks centered at $2\theta \cong 12°$ and $2\theta \cong 17.8°$ were observed in the XRD pattern of TR/β-CD-IC (Figure 4a) owing to channel-type packing of β-CD, which indicated the inclusion complexation of TR with β-CD.[14] However, along with the β-CD peaks, the sharp diffraction peak of TR centered at $2\theta \cong 8.2°$ was also present in the XRD pattern of TR/β-CD-IC because of the existence of some uncomplexed TR in this sample. The DSC analyses, which will be discussed in the following section, also confirmed the presence of free TR in the TR/β-CD-IC sample. In the case of the XRD pattern of TR/γ-CD-IC (Figure 4a), a major peak at $2\theta \cong 7.6°$ and minor diffractions at $2\theta \cong 14.4°$, 15°, 16°, 16.9°, and 22° were observed, confirming the tetragonal channel-type packing of γ-CD.[35,36] In addition, the absence of the TR peak at $2\theta \cong 8.2°$ indicated that complete complexation was achieved between TR and γ-CD. In short, the XRD data revealed that some of the TR used for the preparation of TR/β-CD-IC could not complex with β-CD, whereas all the TR used for the preparation of TR/γ-CD-IC was fully complexed with γ-CD.

The solid TR/β-CD-IC and TR/γ-CD-IC were further characterized by DSC, which is a useful technique to verify whether or not the guest molecules are included inside the CD cavities.[37,38] Typically, if any uncomplexed guest molecules are present in the CD-IC systems, the melting point (T_m) of guest molecules is observed in DSC thermograms of CD-IC.[14,38,39] The DSC thermograms of pure TR and solid TR/β-CD-IC and TR/γ-CD-IC are given in Figure 5. The melting point of pure TR

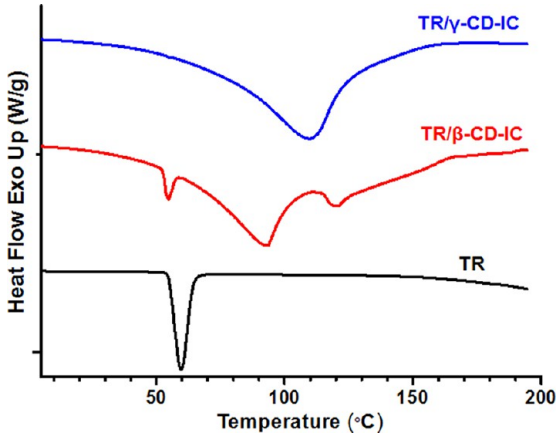

Figure 5. DSC thermograms of pure TR and solid TR/CD-IC.

was observed at 59 °C. The small endothermic peak at around 55 °C was also observed in the DSC thermogram of TR/β-CD-IC, indicating the presence of some free TR in this sample. These DSC data correlate with the XRD data of TR/β-CD-IC having a diffraction peak of some uncomplexed TR crystals. However, the melting peak of free TR was absent in the DSC thermogram of TR/γ-CD-IC, elucidating that the TR was fully complexed with

dx.doi.org/10.1021/jf400440b | J. Agric. Food Chem. 2013, 61, 3901−3908

the γ-CD. Correspondingly, the complete inclusion complexation of TR with γ-CD was also confirmed by the absence of a diffraction peak of TR at $2\theta \cong 8.2°$ in the XRD data of solid TR/γ-CD-IC as discussed in the previous section.

In addition, we investigated the thermal characteristics of TR/β-CD-IC and TR/γ-CD-IC by TGA. TGA studies of CD and pure TR were also performed for comparison. The TGA curve of CD had two weight losses, below 100 °C and above 300 °C, corresponding to water loss and main degradation of CD, respectively (Figure 6a). The TGA thermogram of pure TR

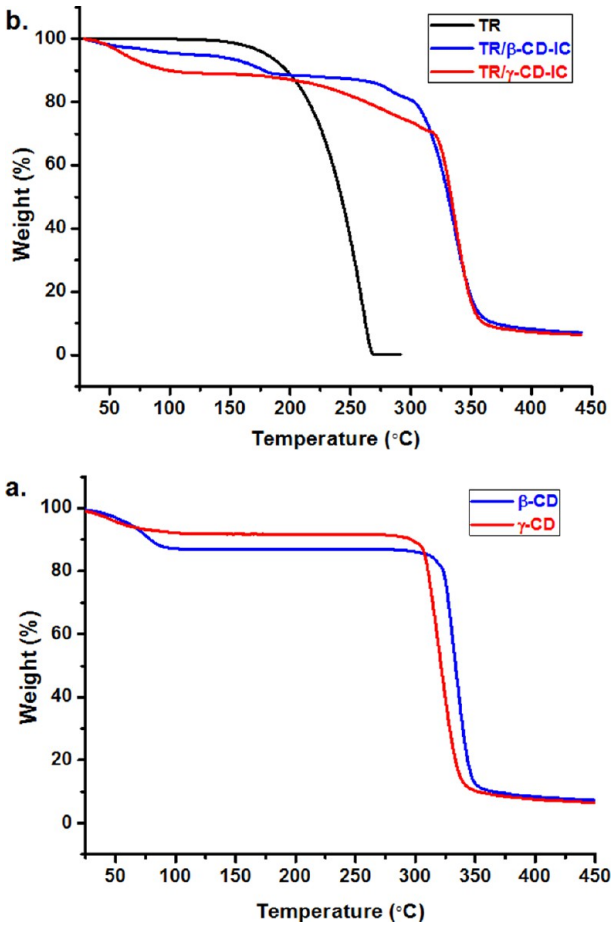

Figure 6. TGA thermograms of (a) as-received CD and (b) pure TR and solid TR/CD-IC.

indicated one major weight loss in the range of 120−270 °C (Figure 6b). The water loss below 100 °C and the main degradation of CD above 300 °C were also observed in TGA thermograms of CD/TR-IC samples (Figure 6b). Yet, additional weight losses due to the evaporation/degradation of TR were present in these samples. For TR/β-CD-IC, the weight loss of TR was observed in two steps; initial weight loss between 120 and 205 °C was owing to uncomplexed free TR molecules. The second weight loss corresponding to the degradation of complexed TR with β-CD occurred at above 275 °C up to 315 °C, at which the main degradation of CD also occurred, indicating the higher thermal stability of TR due to the inclusion complexation. In general, the host−guest interactions in CD-IC increase the thermal stability of the guest molecules included in the CD cavity.[14,40,41] The amount of uncomplexed TR was calculated as ~6% (w/w, with respect to TR/β-CD-IC) from the TGA thermogram of TR/β-CD-IC. The amount of TR in TR/β-CD-IC was determined as ~20% (w/w) from the stoichiometric ratio of TR to β-CD (1:1); therefore, around 70% (w/w) of TR was in the complex state with β-CD in TR/β-CD-IC. In the case of TR/γ-CD-IC, thermal degradation/evaporation of TR took place between 200 and 325 °C, which was much higher than that of the pure TR. In brief, it was observed that the thermal stability of complexed TR was shifted to a much higher temperature due to stronger interaction between TR and the CD cavity in the CD-IC.

In the next part of this study, the incorporation of TR/β-CD-IC and TR/γ-CD-IC in PLA nanofibers was achieved by electrospinning of the solution mixture of PLA and TR/CD-IC. For comparison, PLA and PLA/TR nanofibers were also produced via electrospinning under the same conditions. The representative SEM images of the resulting nanofibers are depicted in Figure 7. Uniform and bead-free nanofibers were

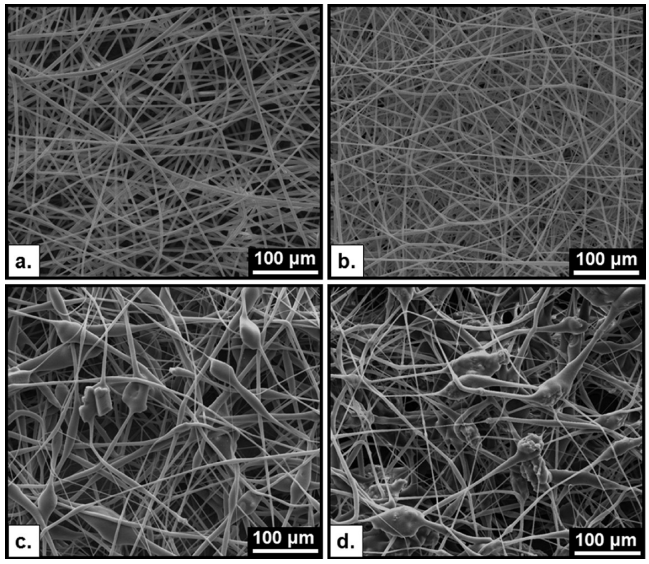

Figure 7. Representative SEM images of the electrospun nanowebs obtained from solutions of (a) PLA, (b) PLA/TR, (c) PLA/TR/β-CD-IC, and (d) PLA/TR/γ-CD-IC.

obtained from PLA and PLA/TR. However, the nanofibers were not uniform in the case of PLA/TR/β-CD-IC and PLA/TR/γ-CD-IC samples, because the aggregates of TR/CD-IC crystals were present and distributed within the nanofiber matrix as confirmed by XRD results discussed in the following section. The viscosity of the solutions used for the electrospinning and average fiber diameter (AFD) with fiber diameter range of the resulting nanofibers are given in Table 1. The viscosities of PLA and PLA/TR solutions were very similar to each other, and so small variations were observed among the AFD and fiber diameter range of these samples. Higher viscosity was observed for the PLA/TR/CD-IC solutions when compared to pure PLA solution, which is possibly owing to the presence of TR/CD-IC crystals in the PLA solution and/or the interactions between the TR/CD-IC and PLA polymer chains. Therefore, thicker fiber diameters were observed in PLA/TR/CD-IC nanofibers due to less stretching of the solutions having higher viscosity. In addition, the standard deviations of AFD of these nanofibers were higher compared to uniform PLA and PLA/TR nanofibers possibly because of the rather complex structure of PLA/TR/CD-IC nanofibers (Table 1).

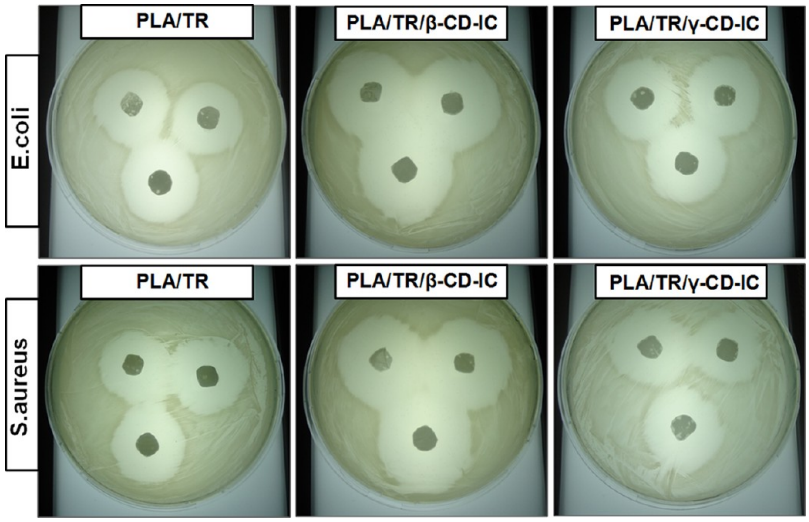

Figure 8. Photographs of antibacterial test of the electrospun nanowebs after 24 h of incubation at 37 °C.

Crystalline structures of the resulting nanowebs of PLA, PLA/TR, and PLA/TR/CD-IC were investigated by XRD (Figure 4b). The XRD pattern of the PLA/TR sample was very similar to that of the PLA nanoweb having a broad diffraction pattern without any characteristic diffraction peaks for TR. This indicated that TR molecules were distributed in the fiber matrix without any crystalline aggregates. Supaphol et al. also reported similar findings, where crystalline drug molecules became amorphous when they were incorporated in electrospun nanofibers.[42] In the case of PLA/TR/CD-IC nanowebs, the diffraction peaks for channel-type packing structure of β-CD and γ-CD were observed in the XRD patterns of PLA/TR/β-CD-IC and PLA/TR/γ-CD-IC nanowebs, respectively. The XRD data confirmed that channel-type packing of TR/CD-IC was well preserved during the solution preparation and electrospinning process and that these crystalline aggregates of TR/β-CD-IC and TR/γ-CD-IC were dispersed within the PLA nanofiber matrix. This result correlates with SEM images that clearly revealed the presence of TR/CD-IC crystalline aggregates in PLA nanofibers.

Antibacterial activities of PLA/TR, PLA/TR/β-CD-IC, and PLA/TR/γ-CD-IC nanowebs were tested against Gram-positive bacteria, *S. aureus*, and Gram-negative bacteria, *E. coli*. As given in Figure 8, the PLA/TR nanoweb caused an inhibition in the growth of both *S. aureus* and *E. coli* due to the well-known antibacterial property of TR. More importantly, the inhibition zones were wider for the PLA/TR/CD-IC nanowebs, suggesting that both PLA/TR/β-CD-IC and PLA/TR/γ-CD-IC nanowebs have better antibacterial properties compared to the PLA/TR system (Table 1). Similar results were also reported by Tonelli et al., where TR/β-CD crystals incorporated in poly(ϵ-caprolactone) (PCL) films have shown improved effectiveness against *E. coli* when compared to PCL film with TR only.[43] This is possibly because of the enhanced solubility of TR into agar medium by CD-IC. It was also noted that the PLA/TR/β-CD-IC sample had better inhibition levels against both of the bacteria when compared to the PLA/TR/γ-CD-IC sample, and this may be caused by the presence of uncomplexed TR in the PLA/TR/β-CD-IC sample, which can be released readily at the initial stage.

In conclusion, we successfully incorporated TR/CD-IC into electrospun PLA nanofibers to obtain nanofibrous webs having antibacterial property. TR did not form an inclusion complex with α-CD; however, the complexation of TR with β-CD and γ-CD was successful, and a 1:1 molar ratio of TR to CD was determined. By forming CD-IC, higher thermal stability was achieved for TR. More importantly, PLA/TR/CD-IC nanowebs have shown better antibacterial activity against *S. aureus* and *E. coli* when compared to a PLA/TR nanoweb, because CD-IC can increase the solubility of TR, which resulted in efficient release of this antibacterial agent from the nanowebs. PLA is a bioderived biodegradable thermoplastic aliphatic polyester, which is applicable in food packaging; therefore, PLA/TR/CD-IC electrospun nanowebs having very high surface area and nanoporous structure as well as having efficient antibacterial property facilitated by TR/CD-IC may be applicable in active food packaging.

AUTHOR INFORMATION

Corresponding Author

*E-mail: tamer@unam.bilkent.edu.tr. Phone:(+90) 312 290 3571. Fax:(+90) 312 266 4365.

Funding

T.U. acknowledges The Scientific and Technological Research Council of Turkey (TUBITAK) (Project 111M459) and EU FP7-PEOPLE-2009-RG Marie Curie-IRG (Project PIRG06-GA-2009-256428, NANOWEB) for funding. We also acknowledge the State Planning Organization (DPT) of Turkey for support of UNAM-Institute of Materials Science and Nanotechnology. F.K. acknowledges TUBITAK-BIDEB for the national Ph.D. study scholarship.

Notes

The authors declare no competing financial interest.

REFERENCES

(1) Greiner, A.; Wendorff, J. H. Electrospinning: a fascinating method for the preparation of ultrathin fibers. *Angew. Chem., Int. Ed.* **2007**, *46* (30), 5670−5703.

(2) Ramakrishna, S.; Fujihara, K.; Teo, W. E.; Yong, T.; Ma, Z.; Ramaseshan, R. Electrospun nanofibers: solving global issues. *Mater. Today* **2006**, *9* (3), 40−50.

(3) Li, D.; Xia, Y. Electrospinning of nanofibers: reinventing the wheel? *Adv. Mater.* **2004**, *16* (14), 1151−1170.

(4) Ramakrishna, S. *An Introduction to Electrospinning and Nanofibers*; World Scientific Publishing: Singapore, 2005.

(5) Wendorff, J. H.; Agarwal. S.; Greiner, A. *Electrospinning: Materials, Processing, and Applications*; Wiley-VCH: Weinheim, Germany, 2012.

(6) Vega-Lugo, A. C.; Lim, L. T. Controlled release of allyl isothiocyanate using soy protein and poly(lactic acid) electrospun fibers. *Food Res. Int.* **2009**, *42* (8), 933−940.
(7) Brahatheeswaran, D.; Mathew, A.; Aswathy, R. G.; Nagaoka, Y.; Venugopal, K.; Yoshida, Y.; Maekawa, T.; Sakthikumar, D. Hybrid fluorescent curcumin loaded zein electrospun nanofibrous scaffold for biomedical applications. *Biomed. Mater.* **2012**, *7* (4), 045001.
(8) Kriegel, C.; Kit, K.; McClements, D.; Weiss, J. Nanofibers as carrier systems for antimicrobial microemulsions. Part I: Fabrication and characterization. *Langmuir* **2008**, *25* (2), 1154−1161.
(9) Fung, W. Y.; Yuen, K. H.; Liong, M. T. Agrowaste-based nanofibers as a probiotic encapsulant: fabrication and characterization. *J. Agric. Food Chem.* **2011**, *59* (15), 8140−8147.
(10) Del Valle, E. M. Cyclodextrins and their uses: a review. *Process Biochem.* **2004**, *39* (9), 1033−1046.
(11) Hedges, A. R. Industrial applications of cyclodextrins. *Chem. Rev.* **1998**, *98*, 2035−2044.
(12) Marques, H. M. C. A review on cyclodextrin encapsulation of essential oils and volatiles. *Flavour Fragrance J.* **2010**, *25* (5), 313−326.
(13) Szejtli, J. Introduction and general overview of cyclodextrin chemistry. *Chem. Rev.* **1998**, *98* (5), 1743−1754.
(14) Kayaci, F.; Uyar, T. Solid inclusion complexes of vanillin with cyclodextrins: their formation, characterization, and high-temperature stability. *J. Agric. Food Chem.* **2011**, *59* (21), 11772−11778.
(15) Samperio, C.; Boyer, R.; Eigel, W. N., III; Holland, K. W.; McKinney, J. S.; O'Keefe, S. F.; Smith, R.; Marcy, J. E. Enhancement of plant essential oils' aqueous solubility and stability using α and β cyclodextrin. *J. Agric. Food Chem.* **2010**, *58* (24), 12950−12956.
(16) Park, I. K.; von Recum, H. A.; Jiang, S.; Pun, S. H. Supramolecular assembly of cyclodextrin-based nanoparticles on solid surfaces for gene delivery. *Langmuir* **2006**, *22* (20), 8478−8484.
(17) Kant, A.; Linforth, R. S. T.; Hort, J.; Taylor, A. J. Effect of β-cyclodextrin on aroma release and flavor perception. *J. Agric. Food Chem.* **2004**, *52* (7), 2028−2035.
(18) Wang, J.; Cao, Y.; Sun, B.; Wang, C. Physicochemical and release characterisation of garlic oil-β-cyclodextrin inclusion complexes. *Food Chem.* **2011**, *127* (4), 1680−1685.
(19) Hădărugă, N. G.; Hădărugă, D. I.; Păunescu, V.; Tatu, C.; Ordodi, V. L.; Bandur, G.; Lupea, A. X. Thermal stability of the linoleic acid/α- and β-cyclodextrin complexes. *Food Chem.* **2006**, *99* (3), 500−508.
(20) Uyar, T.; Hacaloglu, J.; Besenbacher, F. Electrospun polystyrene fibers containing high temperature stable volatile fragrance/flavor facilitated by cyclodextrin inclusion complexes. *React. Funct. Polym.* **2009**, *69* (3), 145−150.
(21) Uyar, T.; Nur, Y.; Hacaloglu, J.; Besenbacher, F. Electrospinning of functional poly (methyl methacrylate) nanofibers containing cyclodextrin-menthol inclusion complexes. *Nanotechnology* **2009**, *20* (12), 125703.
(22) Uyar, T.; Hacaloglu, J.; Besenbacher, F. Electrospun polyethylene oxide (PEO) nanofibers containing cyclodextrin inclusion complex. *J. Nanosci. Nanotechnol.* **2011**, *11* (5), 3949−3958.
(23) Kayaci, F.; Uyar, T. Encapsulation of vanillin/cyclodextrin inclusion complex in electrospun polyvinyl alcohol (PVA) nanowebs: prolonged shelf-life and high temperature stability of vanillin. *Food Chem.* **2012**, *133*, 641−649.
(24) Jug, M.; Kosalec, I.; Maestrelli, F.; Mura, P. Analysis of triclosan inclusion complexes with β-cyclodextrin and its water-soluble polymeric derivative. *J. Pharm. Biomed.* **2011**, *54* (5), 1030−1039.
(25) Qian, L.; Guan, Y.; Xiao, H. Preparation and characterization of inclusion complexes of a cationic β-cyclodextrin polymer with butylparaben or triclosan. *Int. J. Pharm.* **2008**, *357* (1), 244−251.
(26) Du Preez, J.; Yang, W. Improving the aqueous solubility of triclosan by solubilization, complexation, and in situ salt formation. *J. Cosmet. Sci.* **2003**, *54*, 537−550.
(27) Guan, Y.; Qian, L.; Xiao, H. Novel anti-microbial host-guest complexes based on cationic β-cyclodextrin polymers and triclosan/butylparaben. *Macromol. Rapid Commun.* **2007**, *28* (23), 2244−2248.
(28) Veiga, M.; Merino, M.; Cirri, M.; Maestrelli, F.; Mura, P. Comparative study on triclosan interactions in solution and in the solid state with natural and chemically modified cyclodextrins. *J. Incl. Phenom. Macrocycl. Chem.* **2005**, *53* (1), 77−83.
(29) Duan, M. S.; Zhao, N.; Össurardóttir, Í. B.; Thorsteinsson, T.; Loftsson, T. Cyclodextrin solubilization of the antibacterial agents triclosan and triclocarban: formation of aggregates and higher-order complexes. *Int. J. Pharm.* **2005**, *297* (1−2), 213−222.
(30) Vink, E. T. H.; Rabago, K. R.; Glassner, D. A.; Gruber, P. R. Applications of life cycle assessment to NatureWorks polylactide (PLA) production. *Polym. Degrad. Stab.* **2003**, *80* (3), 403−419.
(31) Holm, V. K.; Mortensen, G.; Risbo, J. Quality changes in semi-hard cheese packaged in a poly(lactic acid) material. *Food Chem.* **2006**, *97* (3), 401−410.
(32) Siracusa, V.; Blanco, I.; Romani, S.; Tylewicz, U.; Rocculi, P.; Rosa, M. D. Poly(lactic acid)-modified films for food packaging application: physical, mechanical, and barrier behavior. *J. Appl. Polym. Sci.* **2012**, DOI: 10.1002/app.36829.
(33) Celebioglu, A.; Uyar, T. Electrospinning of polymer-free nanofibers from cyclodextrin inclusion complexes. *Langmuir* **2011**, *27* (10), 6218−6226.
(34) Saenger, W.; Jacob, J.; Gessler, K.; Steiner, T.; Hoffmann, D.; Sanbe, H.; Koizumi, K.; Smith, S. M.; Takaha, T. Structures of the common cyclodextrins and their larger analogues—beyond the doughnut. *Chem. Rev.* **1998**, *98*, 1787−1802.
(35) Rusa, C. C.; Bullions, T. A.; Fox, J.; Porbeni, F. E.; Wang, X.; Tonelli, A. E. Inclusion compound formation with a new columnar cyclodextrin host. *Langmuir* **2002**, *18* (25), 10016−10023.
(36) Uyar, T.; Hunt, M. A.; Gracz, H. S.; Tonelli, A. E. Crystalline cyclodextrin inclusion compounds formed with aromatic guests: guest-dependent stoichiometries and hydration-sensitive crystal structures. *Cryst. Growth Des.* **2006**, *6* (5), 1113−1119.
(37) Koontz, J. L.; Marcy, J. E.; O'Keefe, S. F.; Duncan, S. E. Cyclodextrin inclusion complex formation and solid-state characterization of the natural antioxidants α-tocopherol and quercetin. *J. Agric. Food Chem.* **2009**, *57* (4), 1162−1171.
(38) Giordano, F.; Novak, C.; Moyano, J. R. Thermal analysis of cyclodextrins and their inclusion compounds. *Thermochim. Acta* **2001**, *380* (2), 123−151.
(39) Uyar, T.; El-Shafei, A.; Wang, X.; Hacaloglu, J.; Tonelli, A. E. The solid channel structure inclusion complex formed between guest styrene and host γ-cyclodextrin. *J. Incl. Phenom. Macrocycl. Chem.* **2006**, *55* (1), 109−121.
(40) Marcolino, V. A.; Zanin, G. M.; Durrant, L. R.; Benassi, M. D. T.; Matioli, G. Interaction of curcumin and bixin with β-cyclodextrin: complexation methods, stability, and applications in food. *J. Agric. Food Chem.* **2011**, *59* (7), 3348−3357.
(41) Tsai, Y.; Tsai, H. H.; Wu, C. P.; Tsai, F. J. Preparation, characterisation and activity of the inclusion complex of paeonol with β-cyclodextrin. *Food Chem.* **2010**, *120* (3), 837−841.
(42) Taepaiboon, P.; Rungsardthong, U.; Supaphol, P. Drug-loaded electrospun mats of poly (vinyl alcohol) fibres and their release characteristics of four model drugs. *Nanotechnology* **2006**, *17* (9), 2317.
(43) Lu, J.; Hill, M. A.; Hood, M.; Greeson, D. F.; Horton, J. R.; Orndorff, P. E.; Herndon, A. S.; Tonelli, A. E. Formation of antibiotic, biodegradable polymers by processing with Irgasan DP300R (triclosan) and its inclusion compound with β-cyclodextrin. *J. Appl. Polym. Sci.* **2001**, *82* (2), 300−309.